



UvA-DARE (Digital Academic Repository)

Rising temperature accelerates buoyancy regulation and vertical migration of the bloom-forming cyanobacterium *Microcystis*

Feng, Ganyu; Visser, Petra M.; Huisman, Jef; Verspagen, Jolanda M.H.

DOI

[10.1016/j.watres.2025.124259](https://doi.org/10.1016/j.watres.2025.124259)

Publication date

2025

Document Version

Final published version

Published in

Water Research

License

CC BY

[Link to publication](#)

Citation for published version (APA):

Feng, G., Visser, P. M., Huisman, J., & Verspagen, J. M. H. (2025). Rising temperature accelerates buoyancy regulation and vertical migration of the bloom-forming cyanobacterium *Microcystis*. *Water Research*, 286, Article 124259.
<https://doi.org/10.1016/j.watres.2025.124259>

General rights

It is not permitted to download or to forward/distribute the text or part of it without the consent of the author(s) and/or copyright holder(s), other than for strictly personal, individual use, unless the work is under an open content license (like Creative Commons).

Disclaimer/Complaints regulations

If you believe that digital publication of certain material infringes any of your rights or (privacy) interests, please let the Library know, stating your reasons. In case of a legitimate complaint, the Library will make the material inaccessible and/or remove it from the website. Please Ask the Library: <https://uba.uva.nl/en/contact>, or a letter to: Library of the University of Amsterdam, Secretariat, P.O. Box 19185, 1000 GD Amsterdam, The Netherlands. You will be contacted as soon as possible.

UvA-DARE is a service provided by the library of the University of Amsterdam (<https://dare.uva.nl>)



Rising temperature accelerates buoyancy regulation and vertical migration of the bloom-forming cyanobacterium *Microcystis*

Ganyu Feng^{a,b,c,d}, Petra M. Visser^b, Jef Huisman^b, Jolanda M.H. Verspagen^{b,*}

^a Key Laboratory of Yangtze River Water Environment, Ministry of Education, College of Environmental Science and Engineering, Tongji University, Shanghai 200092, China

^b Department of Freshwater and Marine Ecology, Institute for Biodiversity and Ecosystem Dynamics, University of Amsterdam, Amsterdam 1090 GE, the Netherlands

^c College of Environment, Hohai University, Nanjing 210098, China

^d Present address: College of Biological, Chemical Science and Engineering, Jiaying University, Jiaying 314001, China

ARTICLE INFO

Keywords:

Harmful algal blooms
Lakes
Diurnal vertical migration
Mathematical model
Global warming
Chaos

ABSTRACT

Eutrophication and global warming intensify the formation of harmful cyanobacterial blooms worldwide. Many bloom-forming cyanobacteria can regulate their buoyancy, which results in vertical migration through the water column. Density changes during vertical migration depend largely on carbohydrate production in the light and carbohydrate respiration in the dark, which are temperature-dependent processes. However, the effects of temperature on the vertical migration of *Microcystis* have not been fully investigated yet. Therefore, this study experimentally investigated density regulation at a range of temperatures (17.5, 20, 25 and 30 °C), and developed a mathematical model to predict the temperature-dependent impact of density regulation on vertical migration patterns for colonies of different sizes and in waters with different turbidities. Our experimental results show that elevated temperature enhances carbohydrate production rates in the light and carbohydrate respiration rates in the dark, and thereby accelerates changes in cellular density. Consequently, the model predicts that higher temperature leads to faster migration cycles and increases the number of migration cycles per day. Small colonies display chaotic migration at 17.5 °C, while they synchronize their vertical migration with the day-night cycle in warmer waters. An increasing colony size promotes faster vertical migration, whereas increasing turbidity of the water column reduces migration depth. The modelled migration patterns show that migration at 25 °C yields the highest net daily growth rate. To conclude, our results reveal that rising temperature will accelerate buoyancy changes of *Microcystis*, which modifies their vertical migration patterns and thereby affects the growth and bloom formation of these harmful cyanobacteria.

1. Introduction

Microcystis is one of the most notorious bloom-forming cyanobacteria (Huisman et al., 2018) with a widespread distribution in many eutrophic lakes and reservoirs across the globe (Harke et al., 2016). *Microcystis* can adapt to a wide range of water temperatures from 12 to 30 °C (Xiao et al., 2018), and *Microcystis* blooms seem to be exacerbated by a changing climate (Paerl and Huisman, 2008; Ranjbar et al., 2022). Global warming, and the predicted increase in frequency and intensity of heatwaves in particular (Jöhnk et al., 2008; Witze, 2022), raise questions about the different mechanisms by which temperature may affect *Microcystis* bloom dynamics.

The growth rate of *Microcystis* is highly temperature dependent, with

optimal growth above 25 °C, which exceeds the temperature optimum of many other freshwater phytoplankton species (Roberts and Zohary, 1987; Visser et al., 2016; You et al., 2018). Elevated temperature also increases the stability of the water column (Jöhnk et al., 2008), which benefits buoyant cyanobacteria such as *Microcystis* (Huisman et al., 2004). Furthermore, global warming extends the duration of stratification, with an earlier onset and later cessation of the summer stratification (Woolway et al., 2021) leading to a prolonged blooming period for buoyant cyanobacteria (Wagner and Adrian, 2009). In view of the continued greenhouse gas emissions, *Microcystis* blooms are therefore expected to intensify in the upcoming decades (Visser et al., 2016).

Understanding the different mechanisms by which temperature affects *Microcystis* blooms is of vital importance to make accurate

* Corresponding author.

E-mail address: J.M.H.Verspagen@uva.nl (J.M.H. Verspagen).

<https://doi.org/10.1016/j.watres.2025.124259>

Received 19 March 2025; Received in revised form 13 June 2025; Accepted 18 July 2025

Available online 19 July 2025

0043-1354/© 2025 The Authors. Published by Elsevier Ltd. This is an open access article under the CC BY license (<http://creativecommons.org/licenses/by/4.0/>).

predictions of future bloom dynamics. A key trait of *Microcystis* is that it contains gas vesicles, which provide buoyancy (Walsby, 1994) and give *Microcystis* the ability to migrate vertically through the water column (Kromkamp and Walsby, 1990). Yet, although several studies have investigated the impact of elevated temperature on the population dynamics of *Microcystis* (e.g., Jöhnk et al., 2008), studies that directly assess the impact of temperature on vertical migration are currently lacking.

Vertical migration depends on the density of *Microcystis* cells, which is a function of buoyancy provided by gas vesicles and ballast provided by other cellular components, in particular by carbohydrates (Kromkamp and Mur, 1984). Gas vesicle content usually remains relatively constant during the day, so that density is essentially regulated within hours by the change in cellular carbohydrate content (Thomas and Walsby, 1986). The rate at which carbohydrates are produced in the light depends on photosynthesis, while the rate at which carbohydrates are consumed in the dark depends on respiration (Kromkamp and Walsby, 1990). The regulation of cellular density due to these two processes is known as buoyancy regulation, which has been widely applied to predict vertical migration of *Microcystis* (e.g., Visser et al., 1997; Aparicio Medrano et al., 2013; Wu et al., 2021). Higher temperatures have been reported to have a positive impact on buoyancy regulation in *Microcystis* (Thomas and Walsby, 1986; You et al., 2018). However, how *Microcystis* regulates its density through changes in carbohydrate content at different temperatures is still poorly quantified. Temperature is known to have a positive effect on both photosynthesis and respiration rates in bloom-forming cyanobacteria (Robarts and Zohary, 1987), which is expected to result in increased carbohydrate production as well as increased carbohydrate losses by respiration.

Microcystis cells form colonies (Xiao et al., 2017), which vary in size (Feng et al., 2020). Colony size is known to have a large impact on vertical migration, as larger colonies exhibit higher migration velocities than smaller colonies (Nakamura et al., 1993; Li et al., 2016; Rowe et al., 2016). Furthermore, dense *Microcystis* blooms strongly increase water turbidity, which lowers light availability and induces self-shading (Wu et al., 2021). Since vertical migration is largely driven by light availability, a higher turbidity is expected to impact vertical migration patterns, which in turn feeds back on the formation of dense surface blooms.

This study aims to predict how cellular density changes and vertical migration of *Microcystis* will respond to temperature. For this purpose, we measured the increase in cellular carbohydrate content of *Microcystis* at a range of light intensities and temperatures (17.5, 20, 25 and 30 °C). Furthermore, we measured the decrease in cellular carbohydrate content in the dark along the same temperature range. A vertical migration model adapted from Visser et al. (1997) was parameterized with the temperature-specific experimental data, in order to predict how these density changes impact vertical migration patterns at different temperatures. Furthermore, our model analysis considered different colony sizes of *Microcystis* in waters of different turbidity, to assess interactive effects of temperature, colony size and turbidity on vertical migration patterns and bloom dynamics.

2. The model

Our model simulates the vertical migration of a *Microcystis* colony as a function of changes in cellular carbohydrate content. It is an extension of previous models of the vertical migration of *Microcystis* (Kromkamp and Walsby, 1990; Visser et al., 1997; Aparicio Medrano et al., 2013). Our model includes the effects of temperature on vertical migration in a water column under calm conditions through temperature-dependent parameters. These temperature-dependent parameters include the rates at which carbohydrate is produced by photosynthesis and consumed by respiration, the carbohydrate-specific density of the cells, the cell volume, the cellular gas vesicle content, and the viscosity and density of water.

2.1. Light conditions

The incident light intensity at the water surface (I_{in}) is modeled as a sine function of the time of day (t_d) and day length (D_L):

$$\text{For } D_S \leq t_d \leq D_E : I_{in} = I_{in,max} \sin\left(\frac{\pi(t_d - D_S)}{D_L}\right) \quad (1)$$

$$\text{For } t_d < D_S \text{ and } t_d > D_E : I_{in} = 0$$

where $I_{in,max}$ is the maximum incident light intensity, and D_S and D_E are the start and the end of the light period.

Light intensity in the water column (I_Z) decreases exponentially with depth (Z) according to Lambert-Beer's law, and is a function of the incident light intensity and the total light attenuation coefficient (K_{total}):

$$I_Z = I_{in} \exp(-K_{total}Z) \quad (2)$$

Throughout the manuscript, we will refer to K_{total} as the 'turbidity' of the water column. This turbidity may be caused by, e.g., dissolved organic matter, resuspended sediment or shading by a dense cyanobacterial bloom, but our model does not consider dynamic changes in turbidity (i.e., K_{total} is treated as a fixed model parameter). The euphotic depth (Z_{eu}) is calculated as the depth where light intensity is reduced to 1 % of the incident light intensity (i.e., $Z_{eu} = \frac{\ln(100)}{K_{total}}$).

2.2. Carbohydrate dynamics

The carbohydrate content, Q , of *Microcystis* cells is a dynamic variable, which increases through photosynthesis and decreases through respiration:

$$\frac{dQ}{dt} = P_{I,T} - R_T \quad (3)$$

where the photosynthetic rate $P_{I,T}$ describes the gross carbohydrate production of *Microcystis* as function of light intensity I_Z and temperature T . The light dependence of $P_{I,T}$ is represented by a unimodal function (Visser et al., 1997):

$$P_{I,T} = Y_T I_Z \exp(-I_Z/I_{opt,T}) \quad (4)$$

where Y_T is a scaling parameter. Accordingly, gross carbohydrate production equals zero in the dark (i.e., at $I_Z = 0$), reaches its maximum value at the optimum light intensity $I_{opt,T}$, and asymptotically approaches zero at very high light intensities. Hence, this function allows for photoinhibition of carbohydrate production at high light intensities, as observed in our experiments.

The carbohydrate respiration rate (R_T) is a function of temperature and is described by the Arrhenius equation (Gillooly et al., 2001):

$$R_T = A \exp\left(-\frac{E_A}{k(T+273.15)}\right) \text{ for } Q > Q_{min} \quad (5)$$

$$R_T = 0 \text{ for } Q \leq Q_{min}$$

where A is a normalization constant, E_A is the activation energy, k is Boltzmann's constant, and Q_{min} is the minimum carbohydrate content of the cell. The net carbohydrate production is defined as the difference, $P_{I,T} - R_T$, between the carbohydrate production and respiration rate (i.e. by Eq. (3)).

2.3. Density regulation

The density of cells without gas vesicles ($\rho_{cell,T}$) increases linearly with cellular carbohydrate content according to Visser et al. (1997):

$$\rho_{cell,T} = c_T Q + \rho_{min,T} \quad (6)$$

where c_T is the (temperature-dependent) carbohydrate-specific density and $\rho_{\min,T}$ is the density of cells without gas vesicles and without carbohydrate storage.

The density of the colony $\rho_{\text{colony},T}$ is calculated from $\rho_{\text{cell},T}$ according to Rabouille et al. (2005) and Aparicio Medrano et al. (2013):

$$\rho_{\text{colony},T} = n_{\text{cell}}((1 - n_{\text{gas},T})\rho_{\text{cell},T} + n_{\text{gas},T}\rho_{\text{gas}}) + \rho_{\text{muc}}(1 - n_{\text{cell}}) \quad (7)$$

where n_{cell} is the relative content of cells in the colony, $n_{\text{gas},T}$ is the relative content of gas vesicles in the cells, ρ_{gas} is the density of the gas vesicles, and ρ_{muc} is the density of mucilage. We assume that $\rho_{\text{colony},T}$ cannot become lower than a minimum colony density ($\rho_{\text{col},\min}$) or higher than a maximum colony density ($\rho_{\text{col},\max}$) according to Visser et al. (1997). Therefore, R_T is set to 0 when $\rho_{\text{colony},T} \leq \rho_{\text{col},\min}$, and $P_{I,T}$ is set to 0 when $\rho_{\text{colony},T} \geq \rho_{\text{col},\max}$.

2.4. Vertical migration

The vertical movement of the colony over depth is a function of colony density and based on Stokes' Law (Kromkamp and Walsby, 1990; Visser et al., 1997):

$$\frac{dz}{dt} = u = \frac{2gr^2(\rho_{\text{colony},T} - \rho_{w,T})}{9\Phi\eta_T} \quad (8)$$

where u is the migration velocity, g is the gravitational constant, r is the colony radius, and Φ is the form resistance of the colony. Furthermore, $\rho_{w,T}$ and η_T are the temperature-dependent density and viscosity of water, respectively. In our model, colonies were considered to be sufficiently small to warrant application of Stokes' Law (Aparicio Medrano et al., 2013).

2.5. Specific growth rate

The specific growth rate (μ) was described as a saturating function of the cellular carbohydrate content, according to the Droop equation (Droop, 1973):

$$\mu = \mu_{\max,T}(1 - Q_{\min}/Q) \quad (9)$$

where $\mu_{\max,T}$ is the maximum specific growth rate and Q_{\min} is the minimum carbohydrate content of the cells (i.e., the value of Q at which $\mu = 0$).

We used an iterative algorithm at each time step to solve the differential equations and calculate the migration trajectories of *Microcystis* colonies in a deep water column with a maximum depth of 30 m. Unless stated otherwise, simulations started at the water surface where the colonies were released with initial values of $Z_0 = 0$ m and $Q_0 = Q_{\min}$. Descriptions and units of the model parameters are listed in Supplementary Table S1 and Table S2.

3. Materials and methods

3.1. Strain, growth conditions, and sample analyses

We measured temperature-dependent parameters for the migration model using *Microcystis* strain PCC 7806, kindly provided by the Pasteur Culture Collection (Paris, France). This *Microcystis* strain grew as single cells, not as colonies. *Microcystis* cultures were grown in chemostats, consisting of a flat culture vessel with an optical path length of 5 cm and an effective working volume of 1.8 L, at a dilution rate of 0.12 d⁻¹ (Huisman et al., 2002). The chemostat vessels were illuminated with a day/night cycle of 14 h/10 h from one side by white fluorescent tubes (Philips PL-L 24W/840/4P; Philips Lighting, Eindhoven, The Netherlands) using an incident light intensity of $I_{\text{in}} = 50 \mu\text{mol photons m}^{-2} \text{ s}^{-1}$. The chemostats were supplied with nutrient-rich BG-11

medium (Rippka et al., 1979). The chemostats were maintained at four different temperatures (17.5, 20, 25, and 30 °C) using a metal cooling finger connected to a Cora thermocryostat, and were aerated with sterilized mixed gas with a constant pCO₂ concentration of 400 ppm. The mixed gas was dispersed from the bottom of the chemostat vessel at a gas flow rate of 40 L h⁻¹ using Brooks Mass Flow Controllers.

At each temperature, duplicate chemostat experiments were run (Fig. S1). Two or three times per week, the chemostats were sampled at 9:00 a.m., which was 8 h after the start of the light period. Samples were taken for determination of cell concentration, population biovolume, dry weight, pH, dissolved inorganic carbon (DIC), dissolved inorganic nitrogen (DIN), dissolved inorganic phosphorus (DIP), alkalinity, cell density, cellular carbohydrate content and gas vesicle volume (see Text S1.1 of the Supplementary Materials for methodological details). We used biovolume (i.e. the total volume of all cells) to quantify population size, and expressed carbohydrate content and gas vesicle volume per unit of cell volume. The light intensity was measured with a Model LI-250 light meter (LI-COR Biosciences, Lincoln, Nebraska, USA), at nine spots in front of and behind the chemostat vessels.

3.2. Incubation experiments

At steady state, the specific growth rate and physiological state of the *Microcystis* population in the chemostat are constant and reproducible. For this reason, samples were taken from the steady-state chemostats for a large number of short-term incubation experiments to measure changes in carbohydrate content and cell density at different temperatures and light intensities. Samples (15–20 mL) for these incubations were taken from the chemostats at 9:00 a.m. (i.e., 8 h after the start time of the light period), mixed with fresh BG-11 medium to a total volume of 150 mL, and transferred to small flat Nalgene square bottles (Thermo Fisher Scientific, Massachusetts, USA) with an optical path length of 5 cm for incubation. The incubation flasks were maintained at the same four temperatures as the chemostats, using a metal cooling finger connected to a water bath, and an aeration tube provided mixed gas with a constant pCO₂ concentration of 400 ppm.

The incubations were illuminated by high-intensity halogen light sources approximating the natural daylight spectrum (SoLux MR16-GU5.3/50 W/4P; Tailored Lighting, New York, USA). Different light intensities were obtained by placement of the incubation flasks at different distances from the light source and the use of neutral density filters. The light intensity was measured with the LI-250 light meter at nine spots on the frontside (I_{in}) and backside (I_{out}) of the incubation flasks. Mean light intensity (I_{avg}) was calculated as follows (Huisman et al., 2002):

$$I_{\text{avg}} = \frac{I_{\text{in}} - I_{\text{out}}}{\ln(I_{\text{in}}) - \ln(I_{\text{out}})} \quad (10)$$

In total, for each temperature treatment, *Microcystis* was incubated at 32–52 different mean light intensities ranging from 16.4 to 730.7 $\mu\text{mol photons m}^{-2} \text{ s}^{-1}$ (Fig. S1). To determine the carbohydrate production rate $P_{I,T}$, samples for carbohydrate analysis were taken every 20 min during the first 80 min of the incubation in the light. After exposure to the light for 4 h, the light sources were switched off and samples were taken every 40 to 80 min during the subsequent 4 h dark period to determine the carbohydrate respiration rate R_T from the decrease in carbohydrate content. This gave 32–52 estimates of the carbohydrate respiration rate at each temperature. Samples for population biovolume and cell concentration analysis were taken during the incubations. The carbohydrate production and respiration rates estimated from these incubation experiments were fitted to Eq. (4) and Eq. (5), respectively (see Text S1.2 of the Supplementary Materials for details).

In order to assess the relation between growth rate and carbohydrate content, specified by Eq. (9), we measured cellular carbohydrate content and specific growth rate in 24 h incubation experiments (with a day/night cycle of 14 h/10 h), performed in duplicate at four different

temperatures (17.5, 20, 25, and 30 °C) and four light levels ($I_{\text{avg}} = 38.5 \pm 1.5, 198.6 \pm 5.1, 257.6 \pm 6.2, \text{ and } 375.0 \pm 18.7 \mu\text{mol photons m}^{-2} \text{ s}^{-1}$). Other conditions in these 24 h incubation experiments were kept the same as in the incubation experiments described above. Samples for both population biovolume and carbohydrate content were taken at the beginning and end of these incubations (i.e., at 0 and 24 h). Then, the specific growth rate (μ , in d^{-1}) was calculated as:

$$\mu = \ln(X_{24}/X_0) \quad (11)$$

where X_0 and X_{24} are the population biovolume at the beginning and end of the 24 h incubations, respectively.

3.3. Model scenarios and model analysis

We used the model to simulate long-term vertical migration patterns of *Microcystis* at a range of colony diameters representative of *Microcystis* blooms (100 – 1600 μm ; Li et al., 2013) and lake turbidities common for cyanobacteria-dominated eutrophic lakes (0.8 – 12.4 m^{-1} ; Zhang et al., 2007). Most model parameters, including all temperature-related parameters, were estimated from our experiments, while some model parameters were obtained from the literature (see Text S1.2, Table S1 and Table S2 of the Supplementary Materials for details). The diel variation in incident light intensity was representative for a cloudless summer day with a maximum incident light intensity ($I_{\text{in,max}}$) of 1000 $\mu\text{mol photons m}^{-2} \text{ s}^{-1}$ at solar noon, and had a day length of 14 h (i.e., $D_L=14/24 \text{ d}$). Simulations always ran for at least 35 days, and were only analyzed from day 31 onwards, to get rid of initial transients and allow the carbohydrate dynamics and vertical migration dynamics to get in sync with the fluctuating environmental conditions.

4. Results

4.1. Buoyancy regulation and growth rates

The net carbohydrate production rate increased strongly with light at low light intensities, reached maximum values at light intensities between 262 and 339 $\mu\text{mol photons m}^{-2} \text{ s}^{-1}$, and gradually declined beyond the optimum light intensity (Fig. 1). Both the net carbohydrate production rate at low light intensity and the maximum net carbohydrate production rate increased strongly with increasing temperature

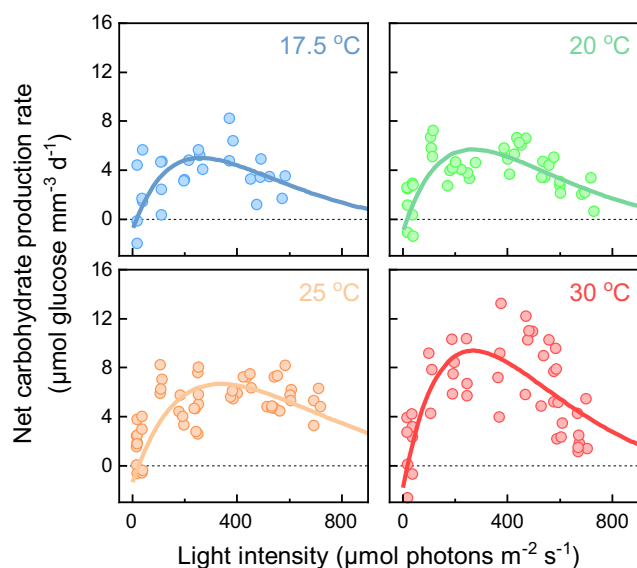


Fig. 1. Net carbohydrate production rate ($P_{I,T}$) as a function of light intensity, at four different temperatures. Solid lines show the fit of Eq. (4) to the data (see Table S3 for statistical details). The parameter values are listed in Table S2.

(Fig. 1). At $I_{\text{opt,T}}$, the maximum net carbohydrate production rate was 5.0, 5.7, 6.7 and 9.4 $\mu\text{mol glucose mm}^{-3} \text{ d}^{-1}$ at 17.5, 20, 25 and 30 °C, respectively, which is equivalent to a temperature coefficient of $Q_{10} = 1.66$ (calculated over the temperature range from 17.5 to 30 °C). Carbohydrate respiration rates in the dark also increased with temperature (Fig. 2a), reaching values of 1.0, 1.1, 1.5, and 1.9 $\mu\text{mol glucose mm}^{-3} \text{ d}^{-1}$ at 17.5, 20, 25 and 30 °C, respectively, which gives a Q_{10} for carbohydrate respiration of 1.67. Carbohydrate-specific density c_T decreased with temperature (Fig. S2), and the volume percent of gas vesicle in the cells was significantly lower at 30 °C than at 20 and 25 °C (Fig. 2b).

The specific growth rate was a saturating function of the cellular carbohydrate content and was well described by the Droop equation (Fig. 3). The minimum carbohydrate content (Q_{min}) was 0.2 $\mu\text{mol glucose mm}^{-3}$ at all four temperatures, whereas the maximum specific growth rate ($\mu_{\text{max,T}}$) estimated by the Droop equation increased from 0.44 d^{-1} at 17.5 °C to 0.94 d^{-1} at 30 °C, which corresponds to a Q_{10} for growth of 1.84.

The values of the temperature-dependent parameters, the statistical analyses, and the steady-state conditions of the chemostat experiments (e.g., cell concentrations, nutrient concentration, pH, alkalinity) are summarized in Tables S2-S5.

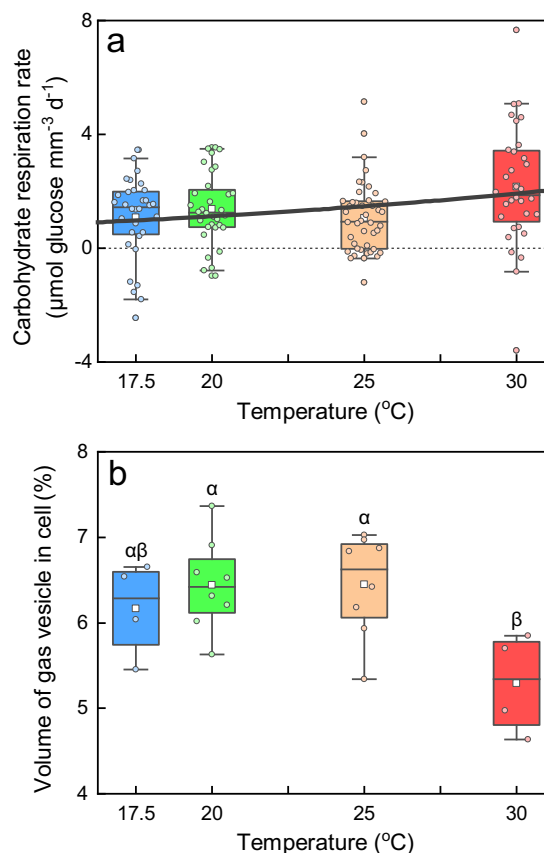


Fig. 2. Carbohydrate respiration and gas vesicle content of *Microcystis* at different temperatures. a: Carbohydrate respiration rate in the dark (R_T). b: Relative gas vesicle content. Box plots show the interquartile range (boxes), mean value (white squares), median value (horizontal lines), 95th and 5th percentiles (error bars), and individual datapoints (small dots). In a, the solid line shows the fit of Eq. (5) to the data (see Table S3 for statistical details). In b, Greek letters (α , β) indicate significant differences in gas vesicle content (based on one-way ANOVA followed by Tukey's HSD test, $p < 0.05$). Parameter values obtained from the data are summarized in Table S2.

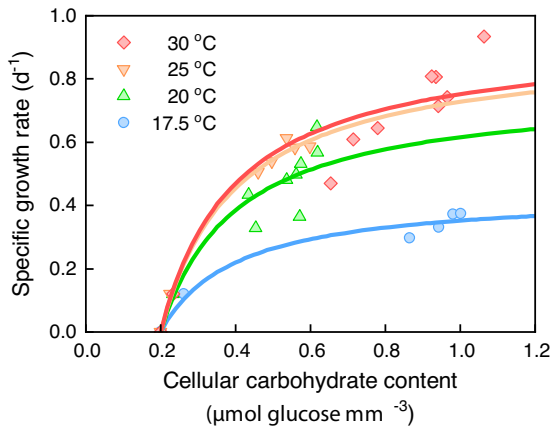


Fig. 3. Specific growth rate (μ) as function of the cellular carbohydrate content (Q). Solid lines show the fit of the Droop equation (Eq. (9)) to the data (see Table S4 for statistical details).

4.2. Vertical migration trajectories

We implemented the temperature dependence of the measured phytoplankton traits in our vertical migration model and studied migration dynamics at a range of conditions. As part of the model analysis, we first studied vertical migration dynamics at a constant incident light intensity (i.e. no day-night cycle) and found that migration patterns depend on incident light intensity, temperature, and initial conditions (i.e. the initial depth, Z_0 , and initial carbohydrate content, Q_0 , when the colonies are released; Fig. 4). At low incident light intensities, colonies display regular oscillations either at or below the

water surface, (Fig. 4a, b). At very high incident light intensities, colonies either become trapped at the water surface because photo-inhibition prevents carbohydrate accumulation (Fig. 4c, d), or display regular oscillation deeper in the water column where light intensities are lower (Fig. 4d). Which of these two states is reached, depends on the initial conditions.

Colonies exposed to a day-night cycle adjust their vertical migration to the daily fluctuations in light availability (Fig. 5). As a consequence, several days after their initial release the vertical migration patterns of colonies with a diameter of 400 μm are no longer dependent on the initial conditions. A few hours after sunrise, the colonies sink due to the photosynthetic accumulation of carbohydrate ballast, which increases their density (Fig. 5b, c, d). Specifically, colonies start their downward journey as soon as their colony density exceeds the temperature-dependent density of water (horizontal dashed lines in Fig. 5c). Because the density of water is higher at lower temperature, colonies at a lower temperature have to accumulate more carbohydrates and reach a higher density before they start sinking (Fig. 5b,c). They return to the water surface after the carbohydrates have been respired in the dark (Fig. 5b, d, e). Colonies start sinking much earlier during the day and return to the water surface much earlier and consequently have shorter migration cycles at high temperature than at low temperature (Fig. 5d, f). This earlier sinking and returning to the water surface at higher temperature is caused by the faster production and respiration rates of cellular carbohydrates at higher temperature (Fig. 5b), and by the lower density of water at higher temperature (Fig. 5c). Hence, in total, these results reveal that colonies in warm waters accumulate carbohydrates faster, will require less carbohydrate ballast in order to start sinking, and will migrate up and down faster than colonies in colder waters.

The model predicts that colony size has a large impact on the migration trajectories of *Microcystis*, by increasing migration velocity and migration frequency (Fig. 6, Fig. S3). Small colonies ($D = 100 \mu\text{m}$)

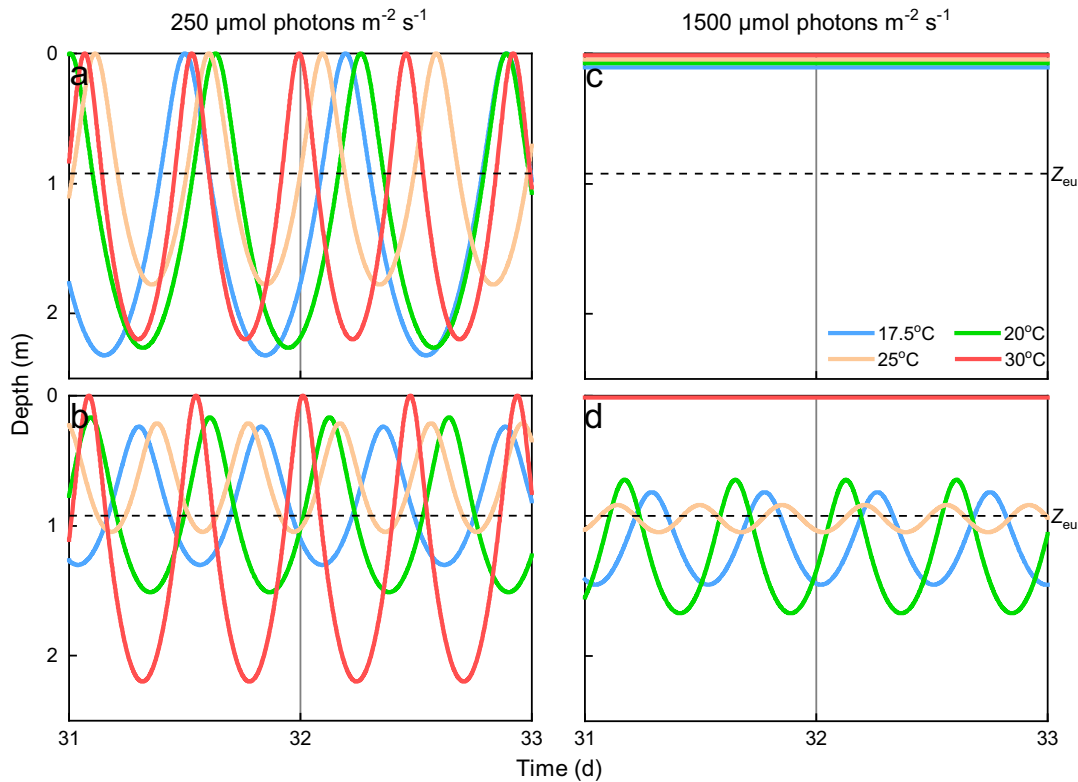


Fig. 4. Simulated migration trajectory of a *Microcystis* colony in continuous light at different temperatures. The migration trajectories of a colony with a diameter of 400 μm at an incident light intensity (I_{in}) of a,b: 250 $\mu\text{mol photons m}^{-2} \text{s}^{-1}$, c,d: 1500 $\mu\text{mol photons m}^{-2} \text{s}^{-1}$. Top panels show migration trajectories with an initial depth $Z_0 = 0 \text{ m}$ and an initial cellular carbohydrate content $Q_0 = Q_{min}$. Bottom panels show migration trajectories with an initial depth $Z_0 = Z_{eu}$ and an initial cellular carbohydrate content $Q_0 = 1.2 \mu\text{mol glucose mm}^{-3}$. In all panels, $K_{total} = 4.4 \text{ m}^{-1}$. The horizontal dashed lines represent the euphotic depth (Z_{eu}).

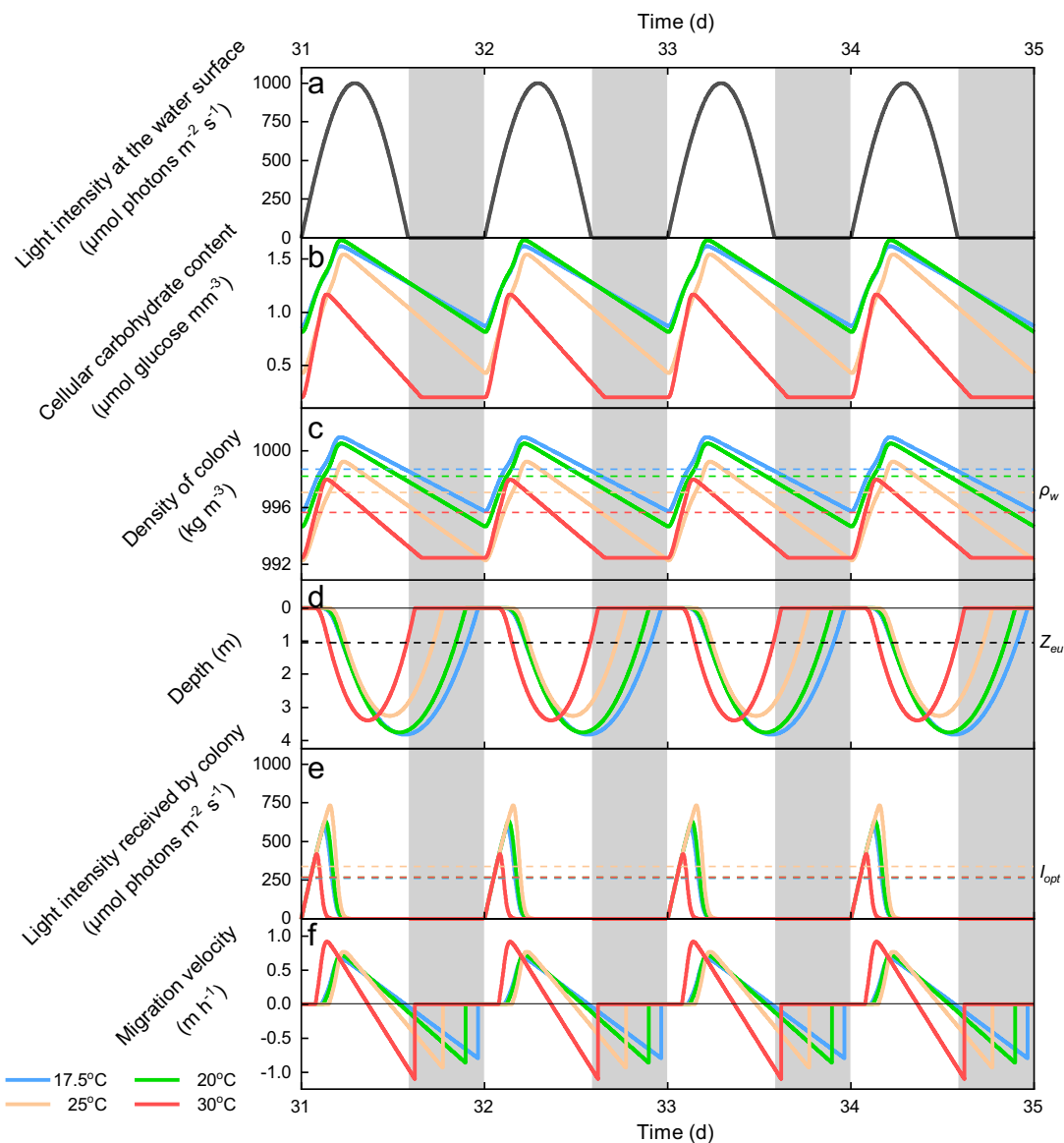


Fig. 5. Simulated migration trajectory of a *Microcystis* colony with a diameter of 400 μm , exposed to a day-night cycle and different temperatures. The dynamics of a: incident light intensity at the water surface, b: cellular carbohydrate content, c: density of colony, d: migration trajectories, e: light intensity received by colony, and f: migration velocities. In all panels, $K_{\text{total}} = 4.4 \text{ m}^{-1}$. Vertical shading indicates nighttime; each day starts with a 14-h light period and ends with a 10-h dark period. Horizontal dashed lines indicate the density of water (ρ_w) at different temperatures in panel c, the euphotic depth (Z_{eu}) in panel d, and the optimal light intensity (I_{opt}) at different temperatures in panel e.

have migration patterns that are irregular and extend over multiple days (Fig. 6b). Slightly larger colonies ($D = 200 \mu\text{m}$) have irregular migration patterns at lower temperature, but regular patterns at higher temperature (Fig. 6c). Large colonies ($D = 800$ and $1600 \mu\text{m}$) display regular diurnal vertical migration patterns at all investigated temperatures, with multiple migration cycles during the day (Fig. 6d, e). Furthermore, migration cycles are shorter and the number of migration cycles per day increases with temperature (i.e. a $1600 \mu\text{m}$ colony completes three cycles at $17.5\text{--}25 \text{ }^\circ\text{C}$, but four cycles at $30 \text{ }^\circ\text{C}$). This can be attributed to higher migration velocities and the earlier onset of vertical migration at $30 \text{ }^\circ\text{C}$ (Fig. 6d-e, Fig. S3e-f).

Migration trajectories are also strongly influenced by the turbidity of the water column (Fig. 7; Fig. S4). Colonies with a diameter of $400 \mu\text{m}$ migrate faster and reach greater depths in clear waters (Fig. 7b), while they stay closer to the surface in turbid waters (Fig. 7c,d). Migration trajectories in clear water at lower temperature are irregular (Fig. 7b). The number of migration cycles increases with temperature and

turbidity.

4.3. Complex dynamics of vertical migration

To investigate in more detail how periodic forcing by the day-night cycle affects vertical migration, we made Poincaré maps (Fig. 8). In these maps, the vertical position and migration velocity of a model colony is plotted once per day, at solar noon, for many consecutive days. Colonies displaying regular daily vertical migration will return to the same vertical position and velocity every day, resulting in a single point on the Poincaré map. Colonies with a periodicity of N days produce N distinct points on the Poincaré map, while colonies with chaotic migration patterns produce a fractal pattern. Fig. 8 illustrates the results for a small colony of $200 \mu\text{m}$. At $17.5 \text{ }^\circ\text{C}$, the time series and Poincaré map are indicative of chaotic vertical migration in which the colony's trajectory varies from day to day (Fig. 8a,b; see Fig. S5 for another example). At 20 and $25 \text{ }^\circ\text{C}$, the colony displays multi-periodic vertical

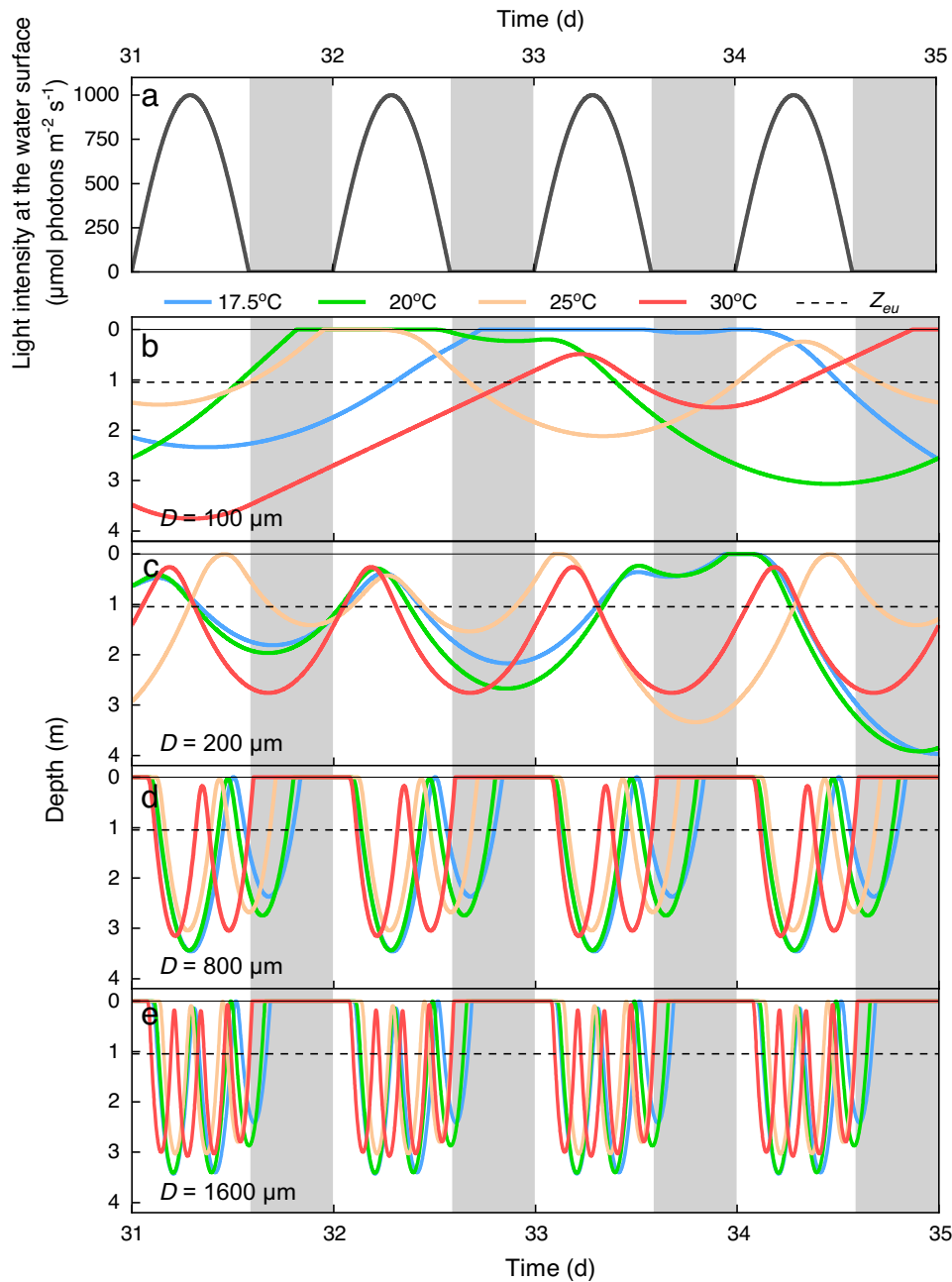


Fig. 6. Simulated migration trajectories of *Microcystis* colonies with different diameters at different temperatures. a: Incident light intensity at the water surface. b-e: Migration trajectories of colonies with a diameter of b: 100 μm , c: 200 μm , d: 800 μm and e: 1600 μm . In all panels, $K_{\text{total}} = 4.4 \text{ m}^{-1}$. Vertical shading indicates nighttime; each day starts with a 14 h light period and ends with a 10 h dark period. The horizontal dashed line in panels b-e indicates the euphotic depth (Z_{eu}).

migration with a repeating pattern every 6 days and every 3 days, respectively (Fig. 8c-f). At 30 °C, the colony displays regular daily vertical migration (Fig. 8g,h). Hence, the dynamics shift from complex migration patterns at 17.5 °C to regular daily migration in warmer waters.

4.4. Daily gains from vertical migration

We explored how net daily growth rate, daily residence time at the water surface (an indication of scum formation), and the number of migration cycles per day of the *Microcystis* colonies are affected by variation in colony diameter and turbidity at different temperatures (Fig. 9). The model predicts that net daily growth rate increases with temperature and is highest at 25 °C, but is not strongly affected by water

turbidity and colony diameter, except at 30 °C (Fig. 9a,f). Small colonies and colonies in clear waters can have multiperiodic and chaotic migration patterns, which cause variation in net daily growth rates as indicated by the scattered distribution of datapoints in Fig. 9. Intermediate-sized and large colonies and colonies in more turbid waters show regular patterns and complete one or more migration cycles per day. The switch from irregular to regular diurnal migration patterns depends on temperature. For example, migration patterns become regular and diurnal at a colony size of $D \geq 380 \mu\text{m}$ at 17.5 °C (Fig. 9b), but already at a colony size of $D \geq 250 \mu\text{m}$ at 30 °C (Fig. 9e).

For colonies with regular diurnal migration, the number of migration cycles increases with temperature, colony size and turbidity (Figs. 6, 7 and 9). Daily residence time at the water surface tends to increase with colony size and turbidity once migration patterns have become regular,

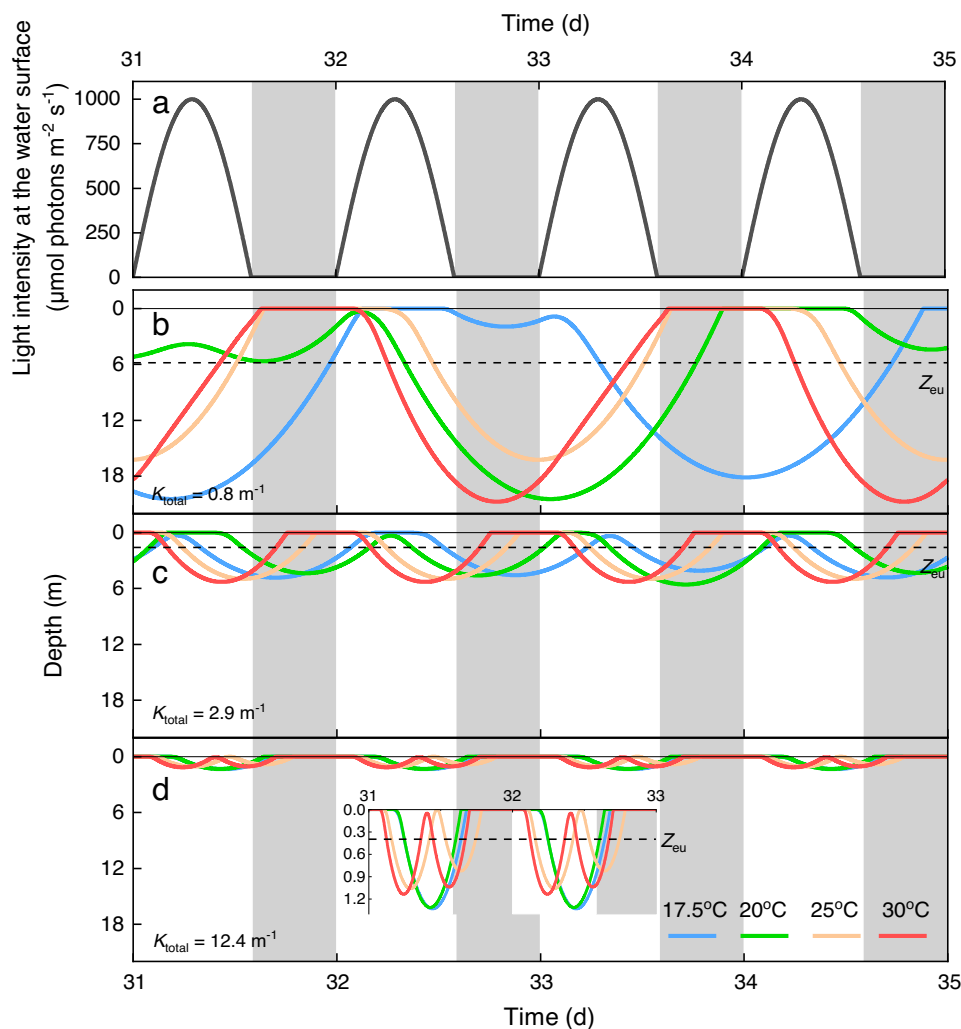


Fig. 7. Simulated migration trajectories of *Microcystis* colonies in waters with different turbidity at different temperatures. a: Incident light intensity at the water surface. b-d: Migration trajectories of colonies at b: low turbidity, c: intermediate turbidity, and d: high turbidity. In all panels, colony diameter is 400 μm . Vertical shading indicates nighttime; each day starts with a 14 h light period and ends with a 10 h dark period. Z_{eu} is the euphotic depth and K_{total} is the total light attenuation coefficient. The insert in panel d is a partial enlargement of trajectories.

but drops at every stepwise increase in the number of migration cycles (Fig. 9b-e,g-j). Maximum migration depth increases with colony size for colonies up to 250 μm , decreases strongly with increasing turbidity, and is hardly affected by temperature (Fig. S6).

5. Discussion

5.1. Effects of temperature on buoyancy regulation and growth

Our experimental results show that both net carbohydrate production in the light and carbohydrate respiration in the dark increased with temperature across the temperature range from 17.5 to 30 $^{\circ}\text{C}$ (Fig. 1; Fig. 2a). These findings are consistent with other studies, which also found an increase of photosynthesis and respiration rates of *Microcystis* spp. across this temperature range (Takamura et al., 1985; Robarts and Zohary, 1987; Coles and Jones, 2000), and temperature optima for photosynthesis of 30 to 35 $^{\circ}\text{C}$ depending on the *Microcystis* strain (Yagi et al., 1994). Furthermore, net carbohydrate production rates estimated by our study had a similar magnitude as in previous studies of Kromkamp and Walsby (1990) and Visser et al. (1997), and resulted in similar changes in cellular density (Fig. S7). Our model results predict that increased rates of carbohydrate production and respiration at elevated temperature will accelerate density changes of *Microcystis* colonies,

which affects their buoyancy regulation. In particular, we found that high temperature increases migration velocities, which shortens the duration of migration cycles and enables large colonies to complete multiple cycles per day.

In addition to carbohydrate accumulation, gas vesicles also have a major effect on the buoyancy of *Microcystis*. However, we found that temperature had little effect on the gas vesicle content of *Microcystis* in the range from 17.5 to 25 $^{\circ}\text{C}$, which is in agreement with Kromkamp et al. (1988) and Visser et al. (1995) who reported a nearly constant relative gas vesicle content between 10 and 20 $^{\circ}\text{C}$. At 30 $^{\circ}\text{C}$, however, gas vesicle content was significantly lower than at 20 and 25 $^{\circ}\text{C}$ (Fig. 2b), consistent with previous observations by Kromkamp et al. (1988) who reported a lower gas vesicle content at 28 $^{\circ}\text{C}$ than at 20 $^{\circ}\text{C}$. Why this high temperature leads to a lower gas vesicle content is not quite clear. Nutrient and light availability, which are often associated with gas vesicle volume (e.g. Brookes and Ganf, 2001), were similar at all temperatures, while other factors (e.g. cell volume; Table S5) showed no clear relation with gas vesicle content.

The growth rate of *Microcystis* is known to be strongly temperature-dependent, with optima usually higher than 25 $^{\circ}\text{C}$ (Robarts and Zohary, 1987; Thomas and Litchman, 2016; Visser et al., 2016). Similar to these previous studies, we found the highest maximum specific growth rates at temperatures of 25 and 30 $^{\circ}\text{C}$ (Fig. 3). High growth rates at elevated

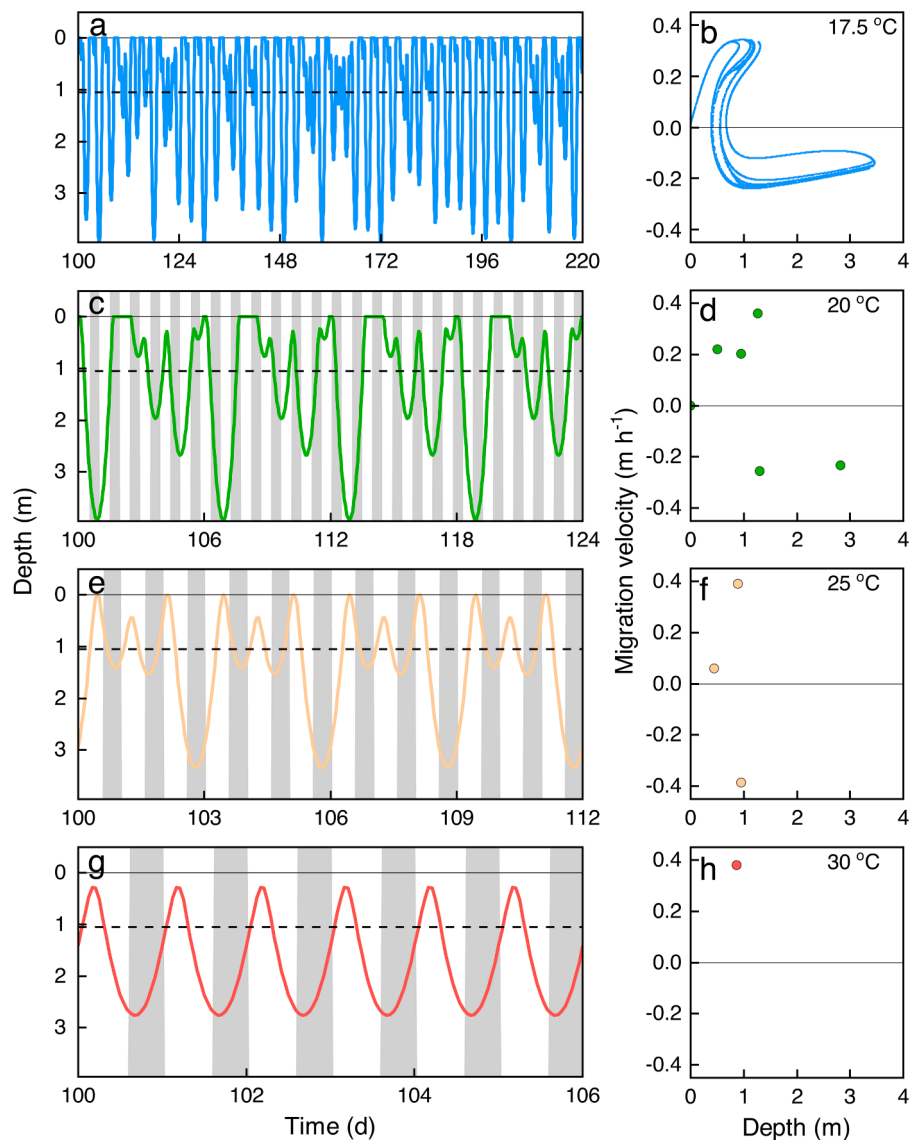


Fig. 8. Time series and Poincaré maps of a *Microcystis* colony at four different temperatures. a,b: 17.5 °C, c,d: 20 °C, e,f: 25 °C, and g,h: 30 °C. Left panels show the vertical migration trajectories for 6–120 days; vertical shading indicates nighttime and the horizontal dashed line represents the euphotic depth (Z_{eu}). Right panels show the corresponding Poincaré map, which plots the vertical position and migration velocity of the colony once every day at solar noon, over a time span of 20,000 days. In all panels, colony diameter is 200 μm and turbidity $K_{total} = 4.4 \text{ m}^{-1}$.

temperature are likely to facilitate the development of dense *Microcystis* blooms (Paerl and Huisman 2008; Visser et al. 2016). However, whereas the maximum specific growth rate was similar at 25 and 30 °C, the model predicts that the net daily growth rate of migrating colonies tends to be highest at 25 °C (Fig. 9a,b). The cellular carbohydrate content at which a colony starts sinking is lower at 30 °C than at 25 °C, because the density of water is lower at 30 °C (Fig. 5b,c). For example, a 400 μm colony adapted to 25 °C only sinks at a carbohydrate content exceeding $1.19 \mu\text{mol glucose mm}^{-3}$, while a similar colony adapted to 30 °C already starts sinking at $0.76 \mu\text{mol glucose mm}^{-3}$. Consequently, migrating colonies at 30 °C have a lower average carbohydrate content than at 25 °C. Since specific growth rate depends on cellular carbohydrate content (Fig. 3), this translates to a lower net daily growth rate at 30 °C than at 25 °C.

5.2. Effects of temperature and other factors on vertical migration patterns

Elevated temperature is known to increase the formation and

development of *Microcystis* blooms (e.g., Paerl and Huisman, 2008; Ranjbar et al., 2022; Li et al., 2023), both by direct effects of temperature on growth rate and by indirect effects of temperature on, e.g., thermal stratification of the water column (Jöhnk et al., 2008; Huisman et al., 2018). Most models concerning the impact of temperature on cyanobacterial blooms focus on the biomass, frequency and intensity of blooms (e.g., Wagner and Adrian, 2009; Cao et al., 2022), rather than on vertical migration. Conversely, most vertical migration models (e.g., Kromkamp and Walsby, 1990; Visser et al., 1997; Aparicio Medrano et al., 2013; Wu et al., 2021) have not investigated effects of temperature.

To our knowledge, one earlier model has studied the impact of temperature on vertical migration of cyanobacteria (Rabouille et al., 2003; 2005). Their model distinguishes between structural cell material and carbohydrate reserves, and differs from our model in how temperature affects some of the metabolic processes (e.g., the basic respiration rate increases with temperature, but the carbon fixation rate is temperature-independent in their model). Furthermore, their model assumes that the carbohydrate production rate of cells decreases with

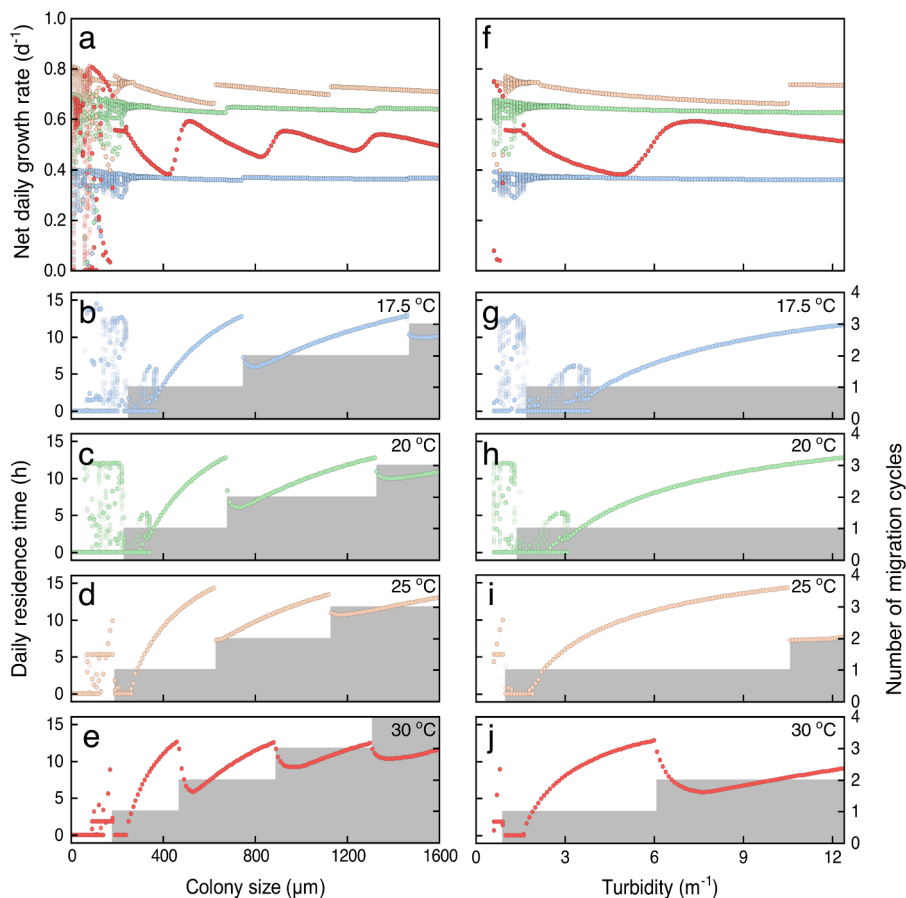


Fig. 9. Model predictions of the impact of colony size and turbidity on net daily growth rate and daily residence time at the water surface at different temperatures. a: Net daily growth rate and b-e: daily residence time at the surface as function of colony size (assuming turbidity $K_{total} = 4.4 \text{ m}^{-1}$). f: Net daily growth rate and g-j: daily residence time at the surface as function of turbidity (assuming a colony size of $400 \mu\text{m}$). The datapoints show daily values from the 31st to 80th day of the simulation, at $17.5 \text{ }^\circ\text{C}$ (blue), $20 \text{ }^\circ\text{C}$ (green), $25 \text{ }^\circ\text{C}$ (orange) and $30 \text{ }^\circ\text{C}$ (red). Scattered datapoints indicate complex dynamics with day-to-day variation in growth rate and residence time. Gray bars represent the number of migration cycles per day.

increasing carbohydrate reserves, which poses a negative feedback on the accumulation of carbohydrate ballast. In continuous light, the vertical migration patterns of the two models differ. The model of Rabouille et al. (2003; 2005) predicts that colonies display vertical migration at low temperatures $< 8 \text{ }^\circ\text{C}$, but settle at a fixed depth in the water column at higher temperatures. In contrast, our model predicts that colonies display vertical migration at all temperatures, unless they become trapped at the water surface at photo-inhibitory light intensities (Fig. 4). These different predictions might be related to the negative feedback on carbohydrate accumulation in the model of Rabouille et al., and the above-mentioned differences in temperature-dependent metabolic processes. When exposed to a day-night cycle, however, both models predict qualitatively similar vertical migration patterns and show a similar dependence on colony size (Rabouille et al. 2005), although chaotic migration patterns have not been reported for their model.

According to our model, *Microcystis* respire part of its carbohydrate storage in the dark, which increases the buoyancy of colonies, and therefore *Microcystis* colonies float to the surface during the night. This is consistent with field observations where the aggregation of *Microcystis* colonies near the water surface tended to increase at night and decrease during the day (Li et al., 2022). Our model predicts that rising temperature will promote higher migration velocities and a quicker return to the water surface (Fig. 6, Fig. 7).

The model predicts that the onset of vertical migration in the morning will be consistently earlier for colonies at $30 \text{ }^\circ\text{C}$, due to a higher carbohydrate production rate (Fig. 1) in combination with a lower density of water at $30 \text{ }^\circ\text{C}$ than at the lower temperatures. The faster

accumulation of carbohydrates results in a faster increase of colony density at $30 \text{ }^\circ\text{C}$ (Fig. 5b,c), while the lower density of water implies that colonies already start sinking at lower colony densities (Fig. 5c,d). We are not aware of laboratory experiments or field observations confirming (or refuting) this temperature-dependent onset of vertical migration.

Furthermore, the model predicts that a large colony size accelerates migration velocity, while high turbidity reduces migration velocity and migration depth. This is consistent with experimental studies that showed that larger colonies migrate faster (Nakamura et al., 1993; Li et al., 2016; Rowe et al., 2016), and aligns with other model studies predicting that increases in turbidity limit the speed and depth of vertical migration (Yao et al., 2017).

5.3. A dynamical systems perspective on vertical migration

An intriguing prediction of our model is that small colonies in clear water show irregular migration patterns, while vertical migration patterns of large colonies and colonies in turbid water are controlled by diurnal variation in light availability (Fig. 9). Chaotic patterns in cyanobacterial migration models have been described before (Sanderson et al., 1992), and recently Yoshiyama et al. (2025) identified that these chaotic dynamics depend on colony size and light availability. Vertical migration of a cyanobacterial colony is an example of a nonlinear oscillating system exposed to periodic forcing by the day-night cycle. It is well known that such systems can display complex dynamics if the natural frequency of the oscillations does not align well with the frequency of periodic forcing (e.g., Rinaldi et al., 1993; Benincà et al.,

2015; Strogatz, 2015). This is the case for small colonies in clear and cold waters, where the natural migration cycle takes longer than the day-night cycle. Large colonies migrate faster, and hence their ups and downs fit within the day-night cycle. This leads to a phenomenon known as ‘frequency locking’ (i.e., the frequency of the migratory oscillations becomes equal to the frequency of external forcing, or integer multiples thereof), where large colonies have synchronized their vertical migration cycle(s) with the day-night cycle. Our model predicts that temperature has a similar effect. That is, higher temperature results in faster carbohydrate dynamics and a faster migration cycle, and therefore small colonies are better able to synchronize their vertical migration with the day-night cycle in warm waters than in cold waters (Fig. 8).

5.4. Extrapolation to the natural situation

Our vertical migration model gives further insights into *Microcystis* bloom dynamics in a warmer world. For example, rising temperature promotes the production of carbohydrates in the light and the respiration of carbohydrates in the dark (Fig. 1, Fig. 2a), and decreases the density of water (Table S2), which shortens the duration of migration cycles and increases the number of migration cycles per day (Fig. 9).

The finding that increasing turbidity will result in a shallower migration depth (Fig. 7) is relevant for the development of cyanobacterial blooms. A growing cyanobacterial population will increase the turbidity of the water column due to self-shading (Huisman et al., 2004; Wu et al., 2021). Hence, vertical migration patterns may alter during the formation of *Microcystis* blooms. Deep vertical migration of *Microcystis* colonies at the onset of the bloom when the water column is still clear and light penetrates deep will help *Microcystis* to avoid photo-oxidative stress or photoinhibition at the water surface (Ibelings, 1996). Shallow vertical migration of the colonies when the turbidity of the water increases during dense blooms will help *Microcystis* to remain in the euphotic zone. As explained by Wu et al. (2021), this may ultimately result in very dense and persistent scums at the water surface, that absorb almost all incident light and display little or no vertical migration.

Our model simulations are representative for calm and sunny weather conditions with very low turbulence in the water column, where *Microcystis* colonies show migration patterns governed by buoyancy regulation. However, conditions in real lakes are more complex and controlled by a range of physical and biological factors. For example, turbulent mixing in lakes is generally highly dynamic and strongly controlled by weather-related processes such as wind-driven currents (Wu et al., 2019), thermal stratification (Facey et al., 2022) and storm intensity (Dai and Nie, 2022). These processes interact with temperature-dependent buoyancy regulation and may disturb the vertical migration of colonies, especially for small colonies (Aparicio Medrano et al., 2013; Zhu et al., 2018).

Buoyancy regulation of cyanobacteria can also be affected by other factors, such as nutrient limitation (Brookes and Ganf, 2001) and fluctuations in incident light intensity by clouds. The size distribution and morphology of colonies can show high variability and complexity not captured by our model (Duan et al., 2018; Cheng et al., 2022). To make more accurate predictions on bloom formation across a wider range of conditions, future studies could extend our model to include nutrient limitation, morphological variability and changes in colony size, fluctuations in incident light intensity, or incorporate our model framework into hydrodynamic models (e.g., Jöhnk et al., 2008) coupled to individual-based models (e.g., Ranjbar et al., 2022).

Furthermore, future studies should aim to combine vertical migration models with field observations (e.g. Aparicio Medrano et al. 2013; Wu et al. 2021; Ranjbar et al. 2022). To the best of our knowledge, studies that compare predicted migration trajectories (e.g. Visser et al. 1997; Rabouille et al. 2005; Yoshiyama et al. 2025) with observed cyanobacterial migration trajectories under natural conditions are still lacking.

6. Conclusions

Our model and experiments improve understanding of the impact of temperature on cyanobacterial blooms, by demonstrating that rising temperature accelerates buoyancy changes of *Microcystis* colonies resulting in faster migration cycles and a larger number of migration cycles per day. Extension of this model to different colony sizes and water turbidities indicates strong interactive effects of temperature, turbidity and colony size on vertical migration patterns. The net daily growth rate of migrating *Microcystis* colonies was predicted to be highest at 25 °C. High growth rates may result in dense cyanobacterial blooms, which promote scum formation at the water surface and deteriorate the water quality of lakes.

Funding

The work was funded by the China Scholarship Council (202006710042).

Data availability

The data and model scripts that support the findings of this study are openly available in figshare. Data are available at [doi:10.21942/uvva.24314395](https://doi.org/10.21942/uvva.24314395). Model scripts are available at [doi:10.21942/uvva.28351193](https://doi.org/10.21942/uvva.28351193).

CRediT authorship contribution statement

Ganyu Feng: Writing – review & editing, Writing – original draft, Visualization, Software, Methodology, Investigation, Funding acquisition, Formal analysis, Data curation, Conceptualization. **Petra M. Visser:** Writing – review & editing, Supervision, Methodology, Conceptualization. **Jef Huisman:** Writing – review & editing, Supervision, Methodology, Formal analysis, Conceptualization. **Jolanda M.H. Verspagen:** Writing – review & editing, Visualization, Supervision, Software, Project administration, Methodology, Investigation, Formal analysis, Data curation, Conceptualization.

Declaration of competing interest

The authors declare that they have no known competing financial interests or personal relationships that could have appeared to influence the work reported in this paper.

Acknowledgments

We thank Rutger van Hall for assistance with the TOC Analyzer, Pieter Slot for DIN and DIP measurements on the autoanalyzer, and Bas van Beusekom for the setup of incubation experiment. We also thank Prof. Wei Zhu from Hohai University for his support in obtaining the funding.

Supplementary materials

Supplementary material associated with this article can be found, in the online version, at [doi:10.1016/j.watres.2025.124259](https://doi.org/10.1016/j.watres.2025.124259).

References

- Aparicio Medrano, E., Uittenbogaard, R.E., Dionisio Pires, L.M., van de Wiel, B.J.H., Clercx, H.J.H., 2013. Coupling hydrodynamics and buoyancy regulation in *Microcystis aeruginosa* for its vertical distribution in lakes. *Ecol. Model.* 248, 41–56.
- Benincà, E., Ballantine, B., Ellner, S.P., Huisman, J., 2015. Species fluctuations sustained by a cyclic succession at the edge of chaos. *Proc. Natl. Acad. Sci. USA* 112 (20), 6389–6394.
- Brookes, J.D., Ganf, G.G., 2001. Variations in the buoyancy response of *Microcystis aeruginosa* to nitrogen, phosphorus and light. *J. Plankton Res.* 23 (12), 1399–1411.
- Cao, H., Han, L., Li, L., 2022. A deep learning method for cyanobacterial harmful algae blooms prediction in Taihu Lake, China. *Harmful. Algae* 113, 102189.

- Cheng, Y., Li, Z., Xiao, Y., Wu, X., Liu, L., 2022. Insights into the role of external layers in cyanobacteria at varying temperatures and their regulatory mechanism. *Freshw. Biol.* 67, 1889–1902.
- Coles, J.F., Jones, R.C., 2000. Effect of temperature on photosynthesis-light response and growth of four phytoplankton species isolated from a tidal freshwater river. *J. Phycol.* 36 (1), 7–16.
- Dai, P.X., Nie, J., 2022. Robust expansion of extreme midlatitude storms under global warming. *Geophys. Res. Lett.* 49 (10), e2022GL099007.
- Droop, M.R., 1973. Some thoughts on nutrient limitation in algae¹. *J. Phycol.* 9 (3), 264–272.
- Duan, Z., Tan, X., Parajuli, K., Upadhyay, S., Zhang, D., Shu, X., Liu, Q., 2018. Colony formation in two *Microcystis* morphotypes: effects of temperature and nutrient availability. *Harmful. Algae* 72, 14–24.
- Facey, J.A., Michie, L.E., King, J.J., Hitchcock, J.N., Apte, S.C., Mitrovic, S.M., 2022. Severe cyanobacterial blooms in an Australian lake: causes and factors controlling succession patterns. *Harmful. Algae* 117, 102284.
- Feng, G., Zhu, W., Xue, Z., Hu, S., Wang, R., Zhao, S., Chen, H., 2020. Structural variations increase the upper limit of colony size of *Microcystis*: implications from laboratory cultures and field investigations. *J. Phycol.* 56 (6), 1676–1686.
- Gillooly, J.F., Brown, J.H., West, G.B., Savage, V.M., Charnov, E.L., 2001. Effects of size and temperature on metabolic rate. *Science* 293 (5538), 2248–2251.
- Harke, M.J., Steffen, M.M., Gobler, C.J., Otten, T.G., Wilhelm, S.W., Wood, S.A., Paerl, H. W., 2016. A review of the global ecology, genomics, and biogeography of the toxic cyanobacterium, *Microcystis* spp. *Harmful Algae* 54, 4–20.
- Huisman, J., Codd, G.A., Paerl, H.W., Ibelings, B.W., Verspagen, J.M.H., Visser, P.M., 2018. Cyanobacterial blooms. *Nat. Rev. Microbiol.* 16 (8), 471–483.
- Huisman, J., Matthijs, H.C.P., Visser, P.M., Balke, H., Sigon, C.A.M., Passarge, J., Weissing, F.J., Mur, L.R., 2002. Principles of the light-limited chemostat: theory and ecological applications. *Antonie Van Leeuwenhoek* 81 (1), 117–133.
- Huisman, J., Sharples, J., Stroom, J.M., Visser, P.M., Kardinaal, W.E.A., Verspagen, J.M., Sommeijer, B., 2004. Changes in turbulent mixing shift competition for light between phytoplankton species. *Ecology* 85 (11), 2960–2970.
- Ibelings, B.W., 1996. Changes in photosynthesis in response to combined irradiance and temperature stress in cyanobacterial surface waterblooms. *J. Phycol.* 32 (4), 549–557.
- Jöhnk, K.D., Huisman, J., Sharples, J., Sommeijer, B., Visser, P.M., Stroom, J.M., 2008. Summer heatwaves promote blooms of harmful cyanobacteria. *Glob. Change Biol.* 14 (3), 495–512.
- Kromkamp, J., Botterweg, J., Mur, L.R., 1988. Buoyancy regulation in *Microcystis aeruginosa* grown at different temperatures. *FEMS Microbiol. Ecol.* 4 (3–4), 231–237.
- Kromkamp, J., Walsby, A.E., 1990. A computer model of buoyancy and vertical migration in cyanobacteria. *J. Plankton Res.* 12 (1), 161–183.
- Kromkamp, J.C., Mur, L.R., 1984. Buoyant density changes in the cyanobacterium *Microcystis aeruginosa* due to changes in the cellular carbohydrate content. *FEMS Microbiol. Lett.* 25 (1), 105–109.
- Li, J., Li, Y., Bi, S., Xu, J., Guo, F., Lyu, H., Dong, X., Cai, X., 2022. Utilization of GOCI data to evaluate the diurnal vertical migration of *Microcystis aeruginosa* and the underlying driving factors. *J. Environ. Manage.* 310, 114734.
- Li, M., Zhu, W., Gao, L., Huang, J., Li, L., 2013. Seasonal variations of morphospecies composition and colony size of *Microcystis* in a shallow hypertrophic lake (Lake Taihu, China). *Fresenius Environ. Bull.* 22 (12), 3474–3483.
- Li, M., Zhu, W., Guo, L., Hu, J., Chen, H., Xiao, M., 2016. To increase size or decrease density? Different *Microcystis* species has different choice to form blooms. *Sci. Rep.* 6, 37056.
- Li, N., Zhang, Y., Zhang, Y., Shi, K., Qian, H., Yang, H., Niu, Y., Qin, B., Zhu, G., Woolway, R.I., Jeppesen, E., 2023. The unprecedented 2022 extreme summer heatwaves increased harmful cyanobacteria blooms. *Sci. Total Environ.*, 165312.
- Nakamura, T., Adachi, Y., Suzuki, M., 1993. Flotation and sedimentation of a single *Microcystis* floc collected from surface bloom. *Water. Res.* 27 (6), 979–983.
- Paerl, H.W., Huisman, J., 2008. Climate - blooms like it hot. *Science* 320 (5872), 57–58.
- Rabouille, S., Salençon, M.-J., Thébault, J.-M., 2005. Functional analysis of *Microcystis* vertical migration: a dynamic model as a prospecting tool. *Ecol. Model.* 188 (2–4), 386–403.
- Rabouille, S., Thébault, J.-M., Salençon, M.-J., 2003. Simulation of carbon reserve dynamics in *Microcystis* and its influence on vertical migration with Yoyo model. *C. R. Biol.* 326 (4), 349–361.
- Ranjbar, M.H., Etemad-Shahidi, A., Helfer, F., Hamilton, D., 2022. Impacts of atmospheric stilling and climate warming on cyanobacterial blooms: an individual-based modelling approach. *Water. Res.* 221, 118814.
- Rinaldi, S., Muratori, S., Kuznetsov, Y., 1993. Multiple attractors, catastrophes and chaos in seasonally perturbed predator-prey communities. *Bull. Math. Biol.* 55 (1), 15–35.
- Rippka, R., Deruelles, J., Waterbury, J.B., Herdman, M., Stanier, R.Y., 1979. Generic assignments, strain histories and properties of pure cultures of cyanobacteria. *Microbiology* 111 (1), 1–61.
- Robarts, R.D., Zohary, T., 1987. Temperature effects on photosynthetic capacity, respiration, and growth rates of bloom-forming cyanobacteria. *N. Z. J. Mar. Freshw. Res.* 21 (3), 391–399.
- Rowe, M.D., Anderson, E.J., Wynne, T.T., Stumpf, R.P., Fanslow, D.L., Kijanka, K., Vanderploeg, H.A., Strickler, J.R., Davis, T.W., 2016. Vertical distribution of buoyant *Microcystis* blooms in a lagrangian particle tracking model for short-term forecasts in Lake Erie. *J. Geophys. Res.* 121 (7), 5296–5314.
- Sanderson, B.G., Webster, I.T., Humphries, S.E., 1992. Chaotic solutions for irradiance-regulated buoyant motion of cyanobacteria. *Limnol. Oceanogr.* 37 (8), 1691–1704.
- Strogatz, S.H., 2015. *Nonlinear Dynamics and chaos: With Applications to physics, biology, Chemistry and Engineering*. CRC Press, Boca Raton, FL.
- Takamura, N., Iwakuma, T., Yasuno, M., 1985. Photosynthesis and primary production of *Microcystis aeruginosa* Kütz. in Lake Kasumigaura. *J. Plankton Res.* 7 (3), 303–312.
- Thomas, M.K., Litchman, E., 2016. Effects of temperature and nitrogen availability on the growth of invasive and native cyanobacteria. *Hydrobiologia* 763 (1), 357–369.
- Thomas, R.H., Walsby, A.E., 1986. The effect of temperature on recovery of buoyancy by *Microcystis*. *Microbiology* 132 (6), 1665–1672.
- Visser, P.M., Ibelings, B.W., Mur, L.R., 1995. Autumnal sedimentation of *Microcystis* spp. As result of an increase in carbohydrate ballast at reduced temperature. *J. Plankton Res.* 17 (5), 919–933.
- Visser, P.M., Passarge, J., Mur, L.R., 1997. Modelling vertical migration of the cyanobacterium *Microcystis*. *Hydrobiologia* 349 (1–3), 99–109.
- Visser, P.M., Verspagen, J.M.H., Sandrini, G., Stal, L.J., Matthijs, H.C.P., Davis, T.W., Paerl, H.W., Huisman, J., 2016. How rising CO₂ and global warming may stimulate harmful cyanobacterial blooms. *Harmful. Algae* 54, 145–159.
- Wagner, C., Adrian, R., 2009. Cyanobacteria dominance: quantifying the effects of climate change. *Limnol. Oceanogr.* 54 (6part2), 2460–2468.
- Walsby, A.E., 1994. Gas vesicles. *Microbiol. Rev.* 58 (1), 94–144.
- Witze, A., 2022. Extreme heatwaves: surprising lessons from the record warmth. *Nature* 608, 464–465.
- Woolway, R.I., Sharma, S., Weyhenmeyer, G.A., Debolskoy, A., Golub, M., Mercado-Bettin, D., Perroud, M., Stepanenko, V., Tan, X., Grant, L., Ladwig, R., Mesman, J., Moore, T.N., Shatwell, T., Vanderkelen, I., Austin, J.A., DeGasperi, C.L., Dokulil, M., La Fuente, S., Mackay, E.B., Schladow, S.G., Watanabe, S., Marcé, R., Pierson, D.C., Thiery, W., Jennings, E., 2021. Phenological shifts in lake stratification under climate change. *Nat. Commun.* 12 (1), 2318.
- Wu, H., Wu, X., Yang, T., Wang, C., Tian, C., Xiao, B., Lorke, A., 2021. Feedback regulation of surface scum formation and persistence by self-shading of *Microcystis* colonies: numerical simulations and laboratory experiments. *Water. Res.* 194, 116908.
- Wu, X., Noss, C., Liu, L., Lorke, A., 2019. Effects of small-scale turbulence at the air-water interface on *Microcystis* surface scum formation. *Water. Res.* 167, 115091.
- Xiao, M., Li, M., Reynolds, C.S., 2018. Colony formation in the cyanobacterium *Microcystis*. *Biol. Rev.* 93, 1399–1420.
- Xiao, M., Willis, A., Burford, M.A., Li, M., 2017. Review: a meta-analysis comparing cell-division and cell-adhesion in *Microcystis* colony formation. *Harmful. Algae* 67, 85–91.
- Yagi, O., Ohkubo, N., Tomioka, N., Okada, M., 1994. Effect of irradiance and temperature on photosynthetic activity of the cyanobacterium *Microcystis* spp. *Environ. Technol.* 15 (4), 389–394.
- Yao, B., Liu, Q., Gao, Y., Cao, Z., 2017. Characterizing vertical migration of *Microcystis aeruginosa* and conditions for algal bloom development based on a light-driven migration model. *Ecol. Res.* 32 (6), 961–969.
- Yoshiyama, K., Sawa, T., Yoshiyama, Y., 2025. Fundamental unpredictability in the vertical migration of cyanobacteria. *Theor. Ecol.* 18 (1), 12.
- You, J., Mallery, K., Hong, J., Hondzo, M., 2018. Temperature effects on growth and buoyancy of *Microcystis aeruginosa*. *J. Plankton Res.* 40 (1), 16–28.
- Zhang, Y., Zhang, B., Ma, R., Feng, S., Le, C., 2007. Optically active substances and their contributions to the underwater light climate in Lake Taihu, a large shallow lake in China. *Fundam. Appl. Limnol.* 170 (1), 11–19.
- Zhu, W., Feng, G., Chen, H., Wang, R., Tan, Y., Zhao, H., 2018. Modelling the vertical migration of different-sized *Microcystis* colonies: coupling turbulent mixing and buoyancy regulation. *Environ. Sci. Pollut. Res.* 25 (30), 30339–30347.